July 2011 Progress Report on

MCNP Modeling for the UMLRR and Selected Gamma Irradiation Facilities

Dr. John R. White, Russell Gocht, and Michael Ducey

Chemical and Nuclear Engineering Department
University of Massachusetts Lowell
Lowell, MA 01854

August 4, 2011

Introduction/Summary

The primary goal of this project is to develop and validate a detailed MCNP model of the UMass-Lowell Research Reactor (UMLRR) to support the analysis of subsequent experiments within the facility. A secondary task is to also develop and validate an MCNP computational model for some of the Co-60 irradiation facilities associated with the UMass-Lowell Radiation Laboratory. This is the 4th update in a series of reports/presentations that will fully document the development of these computational models and provide some summary results of the model validation process for each of the systems treated as part of this project. The previous progress updates (Ref. 1-3) focused primarily on our reactor modeling efforts, with an overview description of the overall MCNP geometry and core layout for the initial LEU startup core (referred to as the M-1-3 model) within the UMLRR.

Since mid-March 2011, we have modified the UMLRR MCNP model to include the experimental bayonets that can be placed in the flux trap and radiation basket locations, updated the treatment of the reference blade location and control blade tip geometry, confirmed the density of reactor grade graphite used within the UMLRR, transitioned to the M-2-5 core configuration including treatment of the first three rows of the excore fast neutron irradiator (FNI) facility, and incorporated a burnup model to account for fuel depletion to the current level of 45-50 MWD of total burnup since the startup of the LEU core in August 2000. In addition, a working model of a standard Co-60 rack surrounded by water has been generated, and some preliminary modeling of this same Co-60 rack on the front face of the gamma cave enclosure has recently been initiated. The goal of this update is to briefly overview these modifications/additions and to pass along some of the MCNP input files containing these new features/capabilities.

Note, however, that much of the final validation testing and model analysis is still underway, so only limited reference to quantitative results is given here. Instead, this update will focus primarily on the model changes that have been made, and the final summary validation results from our studies will be deferred until the Final Project Report -- which should be available in about a month or so. Thus, the remainder of this informal update report will simply expand somewhat on the above list of model enhancements/additions, as follows:

The UMLRR Bayonet Model

Most experimental samples are placed within the core of the UMLRR within an experimental bayonet, which can be flooded or made air tight to keep the samples dry. In both cases, insertion of these elements within a basket location causes a significant local perturbation in the flux, which is

especially true for the case of the dry container. Thus, it is necessary to treat the experimental bayonet explicitly within the MCNP model for proper modeling of the local flux behavior and for correct overall reactivity predictions when one or more bayonets are inserted. For example, the flux mapping measurements within the M-1-3 core had flooded bayonets inserted in positions C2, E2, and D5 and this was not treated in the thermal flux profile comparisons given in Ref. 3, since a bayonet model was not available at that time. Now, with the new MCNP bayonet model, this can be treated properly.

The bayonet is primarily a 1.5″ diameter hollow aluminum tube with a cover and handle that fits nicely into the central aluminum cylinder associated with each experimental radiation basket and flux trap location. The lower portion has a region of lead to counter the buoyancy effects of an empty tube, and experimental samples can be placed within the dry or flooded tube above the lead region for irradiation within the mixed gamma and neutron radiation field at various locations within the reactor. As an example of the model, a sketch of an empty bayonet in D2 and a flooded bayonet in the flux trap in position D5 is illustrated in Fig. 1. This capability now allows for the proper treatment of this experimental facility within all our MCNP models.

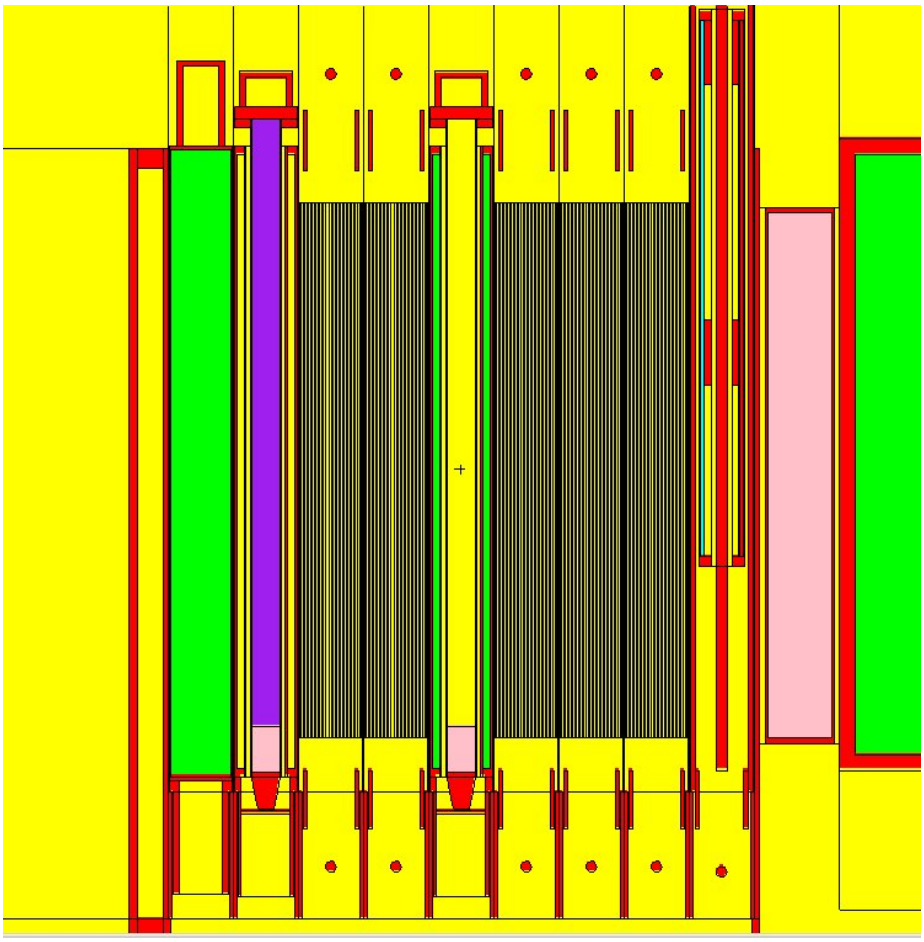

Fig. 1 XZ sketch showing bayonets in positions D2 and D5 of the M-1-3 model (y = 22 cm).

As an example of the affect that a bayonet has on the system, the flux spectrum, with and without an empty bayonet in the central flux trap, is shown in Fig. 2. Here one can clearly see the hardening of the spectrum associated with the removal of water when a dry bayonet is inserted. In addition, since the UMLRR is an over-moderated system and D5 is in the center of the core, this change also leads to a positive reactivity insertion.

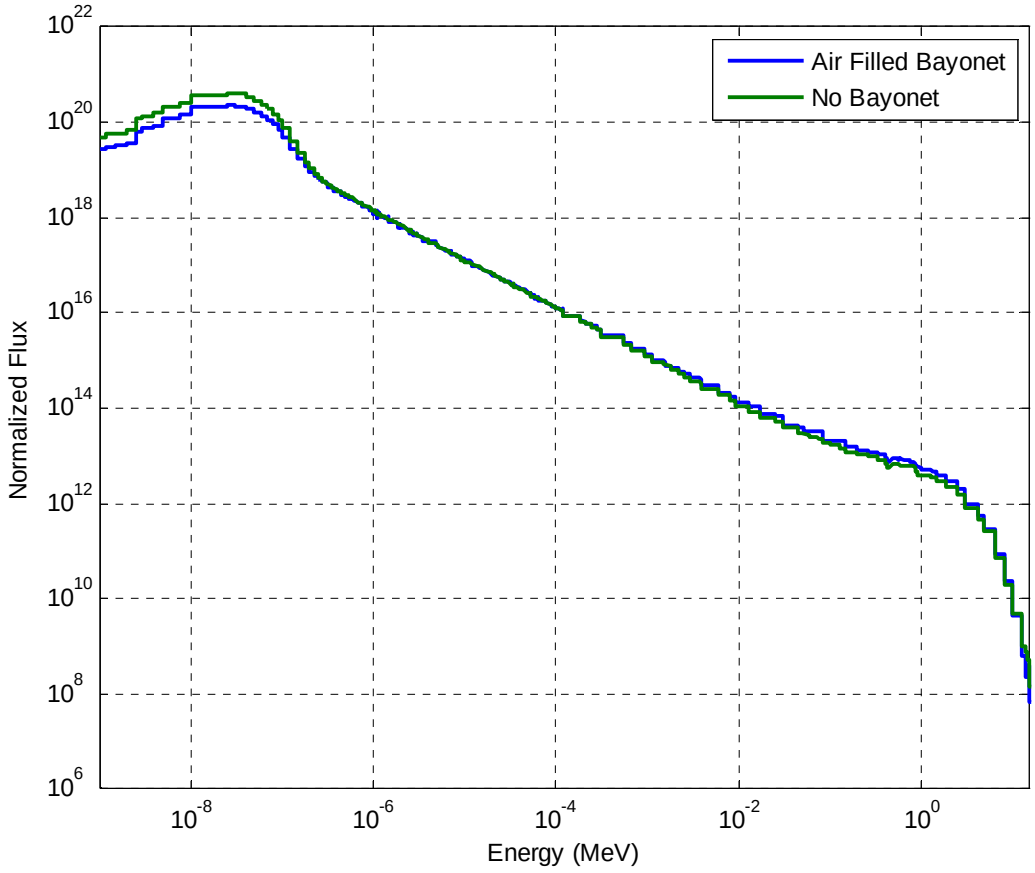

Fig. 2 Normalized flux per unit energy with and without and empty bayonet in position D5.

Changes to the Control Blade Model

In previous progress updates (Refs. 2 and 3), it was noted that the MCNP model computations had a bias of up to -1.5% Δk/k. In an attempt to isolate the cause of this bias, several areas were addressed. In particular, one item of concern was the reference location of the control blades relative to the top of the core grid plate. This quantity was not available from the original reactor drawings and the best information available was that the blade tips were "a couple of inches" above the grid when fully inserted. Thus, in the initial models, a reference height of 2″ above the grid was used as the fully inserted position.

In late June 2011, the UMLRR fuel was off-loaded from the core, the pool drained, and a physical measurement was made of the blade location when fully inserted (see Fig. 3 for a picture of Blade 3 during the measurements). In particular, the distance from the top of the central control blade portion to the top of the shroud was easily measured and, from the reactor blueprints, one can then compute the location of the blade tip in this fully inserted position. All four blades were measured and from these data, one can conclude that the "full-in" position of the blades is about 2.5 inches above the grid plate with an uncertainty of ± 1/8 inch. Thus, all the MCNP models have been changed to make all the blades have the same base level of z = 2.5 inches for full insertion (instead of 2.0 inches in the initial models).

In addition, the lower tip region of the blades has curved edges and this feature was not treated in the original models. In the current models, however, a chamfered edge has been included to conserve the actual blade area in this region in an attempt to model the blade tip region as accurately as possible. A sketch of the new blade model is shown in Fig. 4 within the M-1-3 model at the reference critical height of 15.3″ withdrawn. This blade model will be used in all subsequent MCNP models of the UMLRR.

Sensitivity studies have shown the combined effect of changing the blade tip geometry to that shown in Fig. 4 and moving the reference full-in position to 2.5″ above the grid plate is worth about 0.5% Δk/k -- which helps significantly in reducing the -1.5% Δk/k reactivity bias observed in the original model.

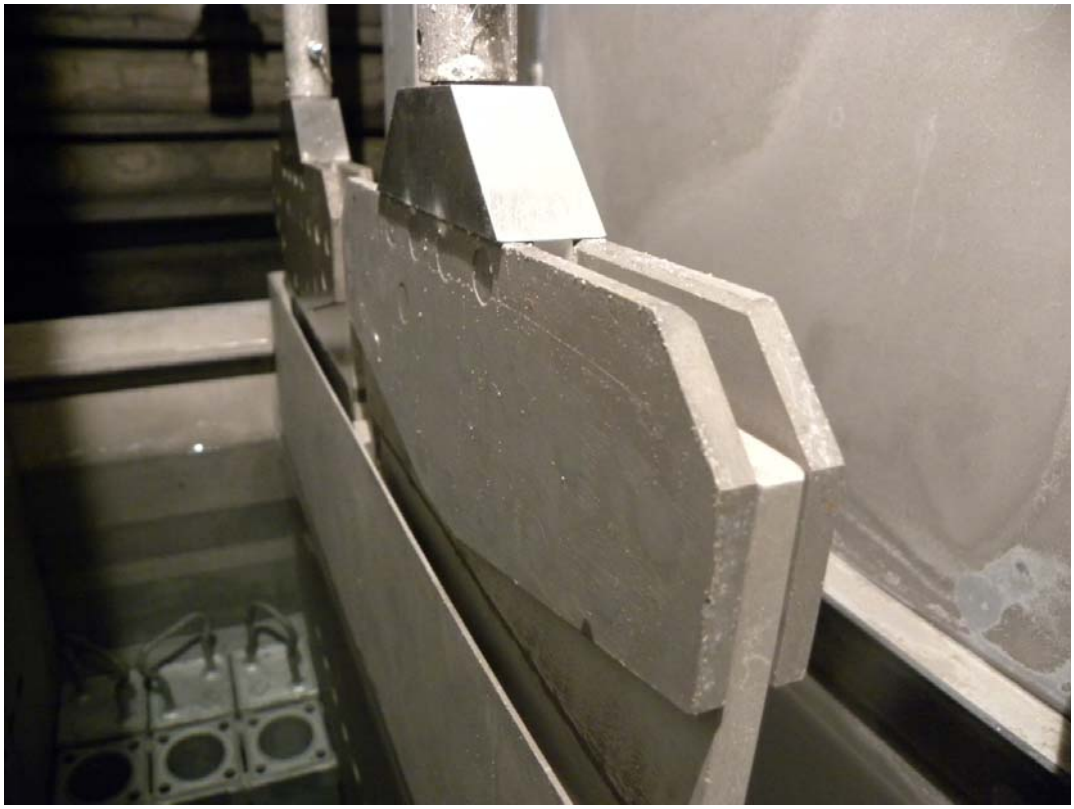

Fig. 3 Picture of Blade 3 showing the top of the central blade region and the top of the control blade shroud. These locations were used to measure the full-in position of the blade tip.

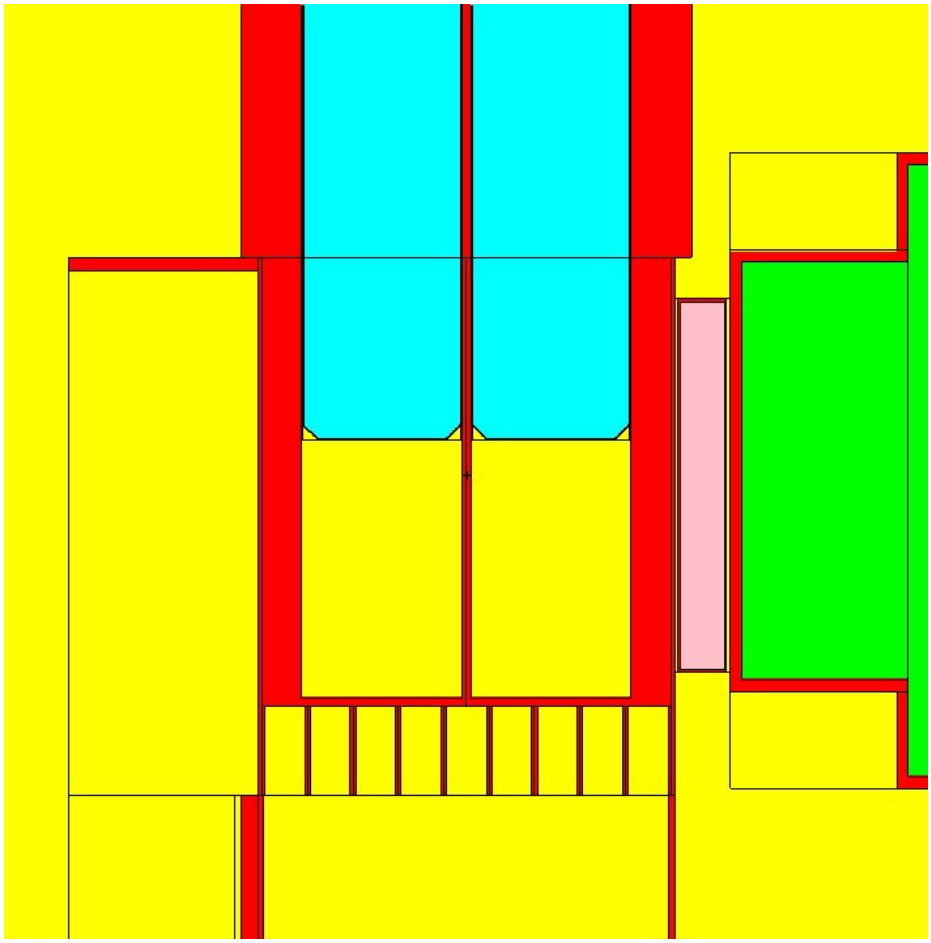

Fig. 4 XZ cut showing the chamfered blade tip geometry in the M-1-3 model (y = 35.5 cm).

On the Density of Reactor-Grade Graphite within the UMLRR

Another item of concern when addressing the original k-bias was the density of the reactor grade graphite used within the UMLRR. The original model used a density of 1.6 g/cm^3, but a quick review of the literature showed a relatively wide range of possible values -- with most of the quoted values varying from slightly less than 1.6 g/cm^3 to slightly greater than 1.8 g/cm^3. A sensitivity study with MCNP showed that an increase in density to 1.8 g/cm^3 would increase k by about 0.5% Δk/k. Although this takes us in the right direction to reduce the original k-bias, we really had no formal basis for making this change.

However, in early July 2011, a sample of the graphite used within the UMLRR was obtained and its density was measured to be about 1.8 g/cm^3. Thus, this was the evidence needed to formally change the reference density from 1.6 to 1.8 g/cm^3 for all future MCNP models of the UMLRR.

Note that, with the combined changes to the blade model and the graphite density, the MCNP value of k for the M-1-3 critical configuration (i.e. Blades 1-4 at 15.3″ withdrawn and the regulating blade at 8″ out) is 0.995, which is certainly much closer to critical than our original model. Note also that ±0.5% Δk/k of unity is considered quite acceptable accuracy for these type of kcode computations in MCNP. Thus, this BOL M-1-3 case is now considered the reference MCNP model for the UMLRR.

The BOL M-2-5 Reference Configuration

The initial emphasis on the M-1-3 startup core for our MCNP model building and validation process is associated with the availability of a variety of experimental measurements for this beginning-of-life (BOL) core configuration -- which is extremely useful for benchmarking purposes. However, the configuration of real interest is the current M-2-5 core. In particular, during the latter part of 2001, an ex-core fast neutron irradiation facility was installed within the UMLRR pool (see Refs. 4 and 5 for details). The purpose of this experimental facility is to provide a large-volume irradiation location that has a relatively high fast neutron flux, with correspondingly low thermal neutron and gamma fluence rates. The fast neutron irradiator (FNI) replaced the three beam ports on the far side of the core in the original M-1-3 startup core (next to row A of the core grid structure). The FNI was purposely placed outside the core region for relatively easy access to the large experimental location and to minimize any effect on core operation during use of this facility. The new irradiation facility did, however, require some changes to the original in-core assembly configuration -- to optimize performance of the FNI and to counter reactivity effects caused by the composite facility changes. Specifically, three key in-core changes were made, including movement of the source holder from grid position A5 to G5, movement of the partial fuel elements from C5 and E5 to C3 and E3, and replacement of five graphite reflectors in row A with newly-designed lead-void assemblies (these elements eliminate the fast neutron moderation associated with graphite and they provide a first level of gamma shielding for the FNI). The resulting configuration, including the FNI grid and shield blocks, is referred to as the M-2-5 configuration and this is also the current operating layout for the UMLRR (in July 2011).

For the current MCNP modeling effort, we are not interested specifically in the FNI facility, but it is indeed important to account for its proximity to the core and its affect on the reactivity and flux distributions within the core. Thus, in the current MCNP models, only those portions of the FNI excore facility that have any affect on the core are modeled with any detail. In particular, only the five Pb-void in-core assemblies in row A and the first three rows of the FNI shield blocks and grid structure are modeled here, since any structure beyond these regions has negligible effect on the in-core neutron and gamma radiation environment.

Several 2-D geometry sketches of the resultant MCNP M-2-5 model are given in Figs. 5 – 7. In particular, Fig. 5 shows the basic in-core assembly layout and the first three rows of the FNI facility next to row A of the core grid in the xy plane at the centerline of the core. Here one can clearly see that the radiation basket used for the startup neutron source has been moved to location G5, that row A contains five new Pb-void elements that were not present in the M-1-3 core, and that the first three rows of the FNI facility outside row A of the core grid contain a staggered set of 3″×6″ and 3″×9″ Pb shield blocks to provide gamma shielding for the fast neutron irradiator experimental region (which is not modeled here). In addition, as shown in Fig. 6, a yz planar view near the core centerline (at x = 11.43 cm) of the same layout, also highlights these same features, but this view shows the axial geometry of the new elements associated with all the post-FNI UMLRR cores.

In brief, the Pb-void elements are about 29″ long and fit in a regular 3″×3″ grid location. Internally, these elements contain about 0.5 inches of lead on either side of an air space within aluminum inner and outer structures. Five of these elements were fabricated and inserted into the central five positions of row A within the core grid. This design provides about 1″ of primary gamma shielding and it also tends to neutronically de-couple the core region from the remainder of the FNI facility. More importantly from the FNI perspective, however, is that these elements do not significantly decrease the fast flux.

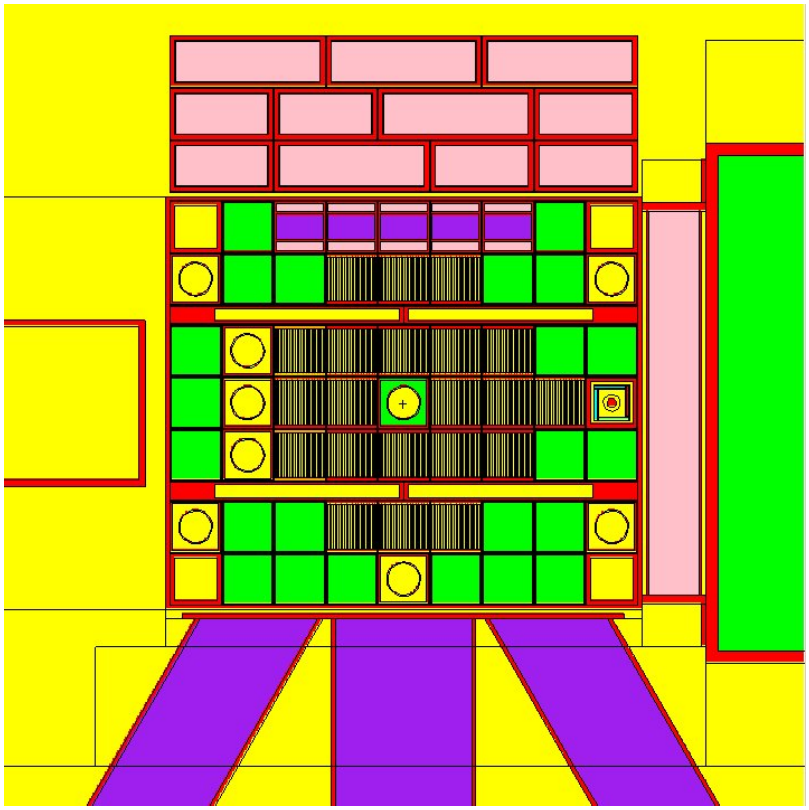

Fig. 5 XY view of the BOL M-2-5 configuration (z = 38.1 cm).

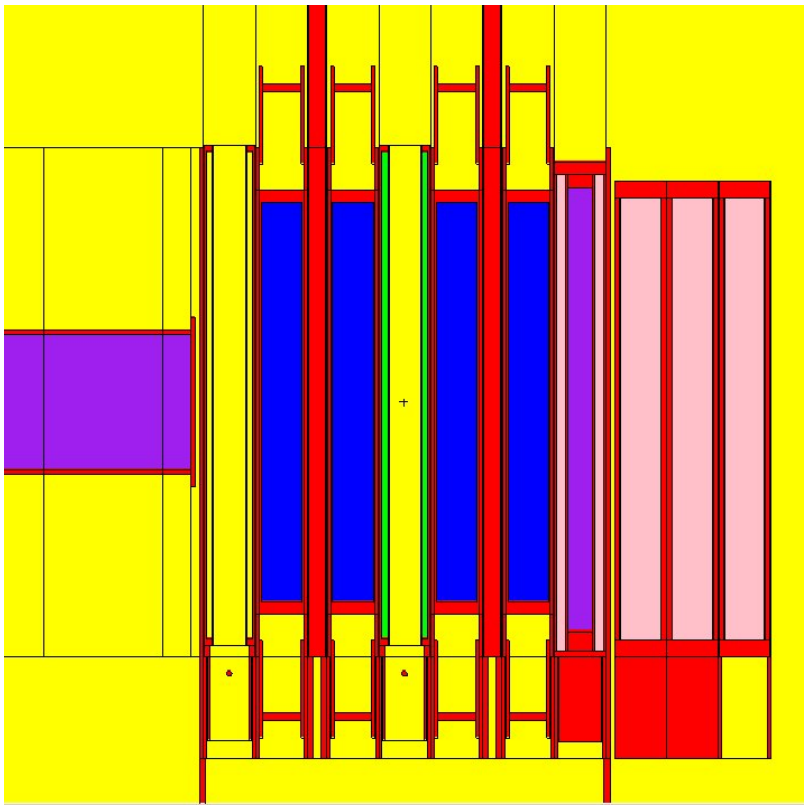

Fig. 6 YZ view of the BOL M-2-5 configuration (x = 11.43 cm).

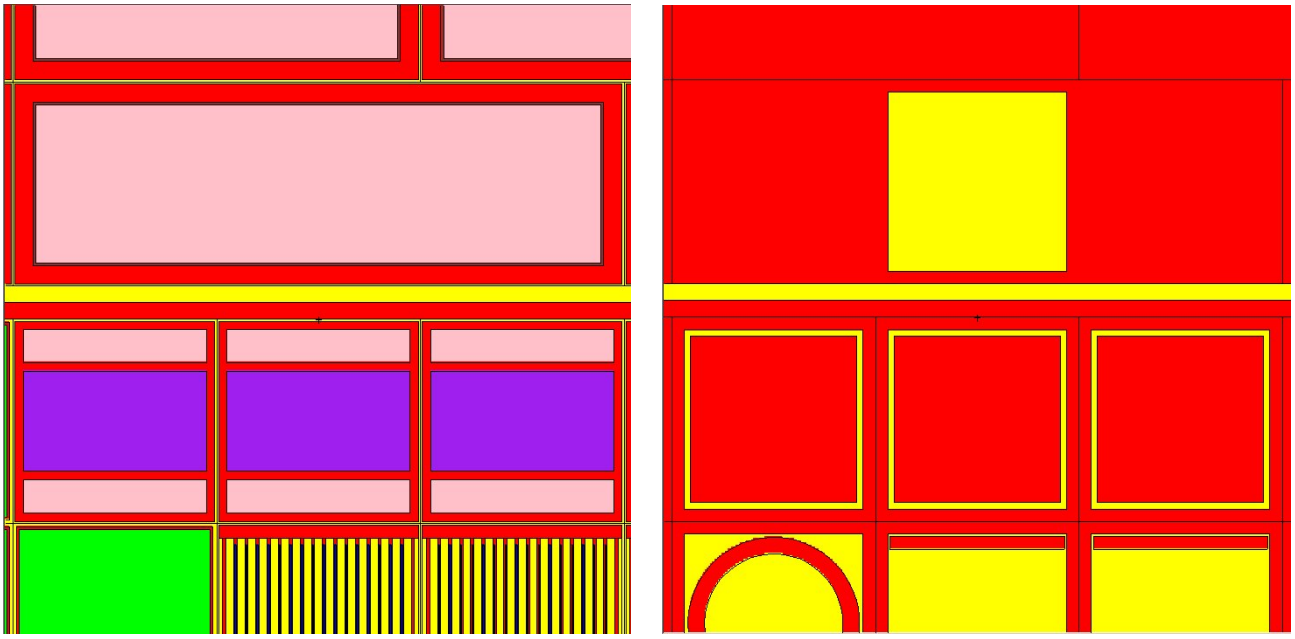

Fig. 7 Expanded local XY views of the new Pb-void and Pb-shield elements in the M-2-5 core. The two sketches show a mid-core elevation (left side) and a grid plate elevation (right side).

For the shield blocks in the excore FNI grid, the Pb in each block is contained within roughly a 1/4″ thick aluminum can that is lined on the inside with a thin sheet of borated aluminum. These blocks have a length of about 28″. A small water gap (between 1/16″ and 1/8″) is needed for cooling and for ease of insertion and removal of the elements. The approximately 2.35″ of lead within each block attenuates the gamma flux from the core and the secondary gammas generated in the water surrounding the FNI grid. The borated aluminum along the inside walls keeps the thermal flux sufficiently low so that secondary gamma generation in the lead is not a problem.

Both the Pb-void elements and the Pb-shield blocks have solid aluminum end boxes that fit into their respective lower grid structures. Note, however, that each Pb-shield block has only two end boxes, so, for the 3″×9″ design, the middle grid location is empty.

Many of the features associated with the new elements within the M-2-5 core are apparent in Figs. 5 and 6. In addition, in Fig. 7, which shows an expanded xy view of only the new elements (centered above location A4), one can also see a few additional details -- such as the thin B-Al liner inside the shield blocks (i.e. the thin brown layer between the pink Pb inner region and the red outer Al can in the left half of Fig. 7), and the treatment of the end boxes as seen in the right half of Fig. 7.

With a complete M-2-5 geometry configuration and BOL element compositions, one can now perform a series of MCNP computations with this model. The reported critical blade heights, for example, for the initial UMLRR M-2-5 configuration had Blades 1-4 at 15″ out and the regulating blade at 10.1″ withdrawn. However, the M-2-5 configuration was actually constructed after a burnup of about 3.7 MWD with the LEU fuel. Thus, based on extrapolated critical height versus burnup data, we estimate that the critical heights for a fresh core load would have been about 14.9” and 10″ respectively, for the large control blades and regulating blade. Thus, these latter values are used in the BOL M-2-5 MCNP model, with a resultant k = 0.999. Thus, this configuration also gives a “critical” k-value that is very close to unity.

The M-2-5 Model with Fuel Depletion

During the approximately 11-year period since startup (Aug. 2000 through June 2011), the LEU core achieved about 1100 MWhr of total burnup (i.e. equivalent to about 45 - 50 full power days at 1 MW operation) -- where we note that the operation of the UMLRR is usually very intermittent and much of it occurs at low power in increments of only a few hours for a variety of training and educational purposes. Historically, because of the relatively low total burnup, most of the physics analysis of the UMLRR performed to date has simply ignored fuel depletion effects, arguing that the flux distributions and reactivity worths are not significantly altered by the relatively mild fuel distribution changes caused by such a low total burnup. However, it is important to note that these depletion effects have never been quantified -- the arguments used represent a general expectation, not a formal quantitative assessment. Thus, since our ultimate goal for this project is a very detailed MCNP model of the current UMLRR configuration (which includes 45- 50 MWD of burnup), one of the important subtasks for this work was to formally assess the importance of fuel depletion in our on-going physics analysis of the UMLRR.

The standard approach to treating depletion in MCNP is to couple the MCNP flux computations with a point burnup code. In particular, for the current study, we obtained the MCODE software from MIT (see Ref. 6) which automatically provides the required linkage between MCNP5 and ORIGEN2.2 to allow for detailed fuel depletion studies within the 3-D explicit geometries available as part of the full MCNP model.

Various levels of approximation are available here, including detailed depletion on a plate-by-plate level with many axial zones. However, to keep the current analysis manageable, a 5-zone axial model was selected with fuel depletion on an assembly-by-assembly basis. Thus, the cell and material descriptions for the 21 fuel assemblies within the BOL M-2-5 core were modified to have a different representation for each assembly and each axial layer -- giving $21 \times 5 = 105$ explicit fuel zones within the depletion-ready MCNP model. The assemblies were numbered 1 through 21 as shown in Fig. 8, and each layer was numbered 1 through 5 going from bottom to top in the axial direction, with the active fuel length broken into five equal axial segments. Only the material within the fuel meat section of the fuel plate/assembly is tagged as depletable, so all the other materials within the reference model remain unchanged.

To illustrate the model changes needed here, a short segment of the actual depletion-ready MCNP input deck is given in Fig. 9 to highlight the naming convention used for the fuel materials, and Fig. 10 contrasts a small portion of two neighboring fuel assemblies for the reference and depletion-ready MCNP models. In particular, Fig. 10 shows the last 5 plates of the fuel assembly in D3 and the first 5 plates in the fuel element in D4. Clearly, one can see that the depletion-ready case has 5 axial regions/materials in each fuel plate and that each assembly has a different material assignment -- which allows for space-dependent material composition changes to be tracked versus burnup. At BOL, all the fuel material compositions are identical in all these regions but, after some amount of depletion, the model now allows for burnup-dependent fuel compositions within the 105 fuel regions specified within the new depletion-ready model.

With this new MCNP geometry model, MCODE was used to deplete the UMLRR M-2-5 core configuration to a burnup of 50 MWD to approximately represent actual current operations in the UMLRR (July 2011). A no-xenon option was implemented, since the UMLRR operational schedule is such that equilibrium xenon is never achieved -- in fact, most operation and experimental testing is done in a near Xe-free environment, except for the small amount of Xe-135

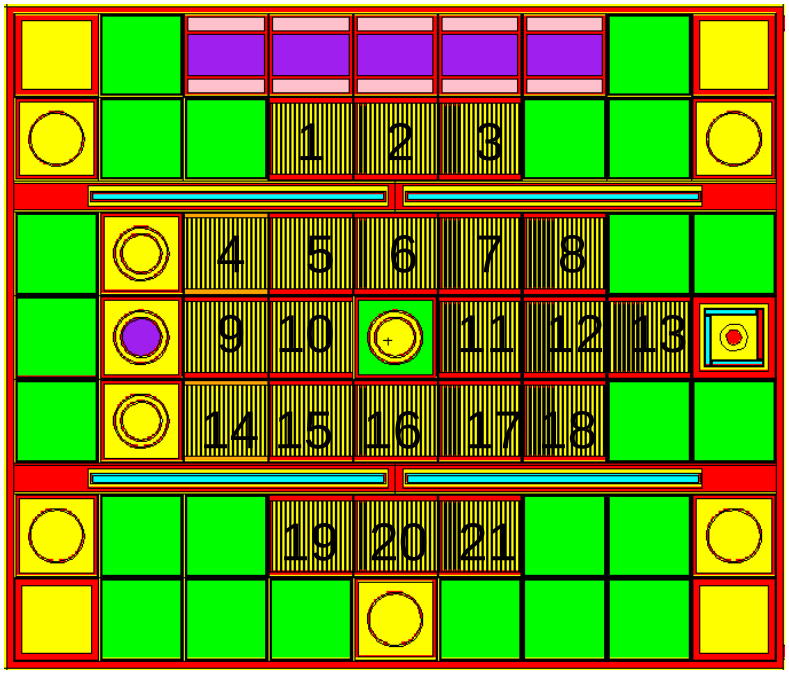

Fig. 8 Assembly numbering scheme for the depletion-capable models.

```
c
c Discrete materials for fuel zones to support depletion calculations
c   convention for material number is RRAPP
c     RR - radial location, 1 to 21, row major order
c     A  - axial location, 1 to 5, bottom to top
c     PP - plate location, 1 to 18, left to right (not yet used)
c     if A=0 or PP=0 then no axial or plate-wise divisions
m1000   92235.70c 1.7291e-3   92238.70c 6.9369e-3   13027.70c 3.9542e-2
        14028.70c 5.3284e-3   14029.70c 2.6980e-4   14030.70c 1.7910e-4
m1100   92235.70c 1.7291e-3   92238.70c 6.9369e-3   13027.70c 3.9542e-2
        14028.70c 5.3284e-3   14029.70c 2.6980e-4   14030.70c 1.7910e-4
m1200   92235.70c 1.7291e-3   92238.70c 6.9369e-3   13027.70c 3.9542e-2
        14028.70c 5.3284e-3   14029.70c 2.6980e-4   14030.70c 1.7910e-4
m1300   92235.70c 1.7291e-3   92238.70c 6.9369e-3   13027.70c 3.9542e-2
        14028.70c 5.3284e-3   14029.70c 2.6980e-4   14030.70c 1.7910e-4
m1400   92235.70c 1.7291e-3   92238.70c 6.9369e-3   13027.70c 3.9542e-2
        14028.70c 5.3284e-3   14029.70c 2.6980e-4   14030.70c 1.7910e-4
m1500   92235.70c 1.7291e-3   92238.70c 6.9369e-3   13027.70c 3.9542e-2
        14028.70c 5.3284e-3   14029.70c 2.6980e-4   14030.70c 1.7910e-4
m2000   92235.70c 1.7291e-3   92238.70c 6.9369e-3   13027.70c 3.9542e-2
        14028.70c 5.3284e-3   14029.70c 2.6980e-4   14030.70c 1.7910e-4
m2100   92235.70c 1.7291e-3   92238.70c 6.9369e-3   13027.70c 3.9542e-2
        14028.70c 5.3284e-3   14029.70c 2.6980e-4   14030.70c 1.7910e-4
m2200   92235.70c 1.7291e-3   92238.70c 6.9369e-3   13027.70c 3.9542e-2
        14028.70c 5.3284e-3   14029.70c 2.6980e-4   14030.70c 1.7910e-4
m2300   92235.70c 1.7291e-3   92238.70c 6.9369e-3   13027.70c 3.9542e-2
        14028.70c 5.3284e-3   14029.70c 2.6980e-4   14030.70c 1.7910e-4
m2400   92235.70c 1.7291e-3   92238.70c 6.9369e-3   13027.70c 3.9542e-2
        14028.70c 5.3284e-3   14029.70c 2.6980e-4   14030.70c 1.7910e-4
m2500   92235.70c 1.7291e-3   92238.70c 6.9369e-3   13027.70c 3.9542e-2
        14028.70c 5.3284e-3   14029.70c 2.6980e-4   14030.70c 1.7910e-4
```

Fig. 9 Portion of MCNP input deck showing material numbering scheme for the depletion-capable models.

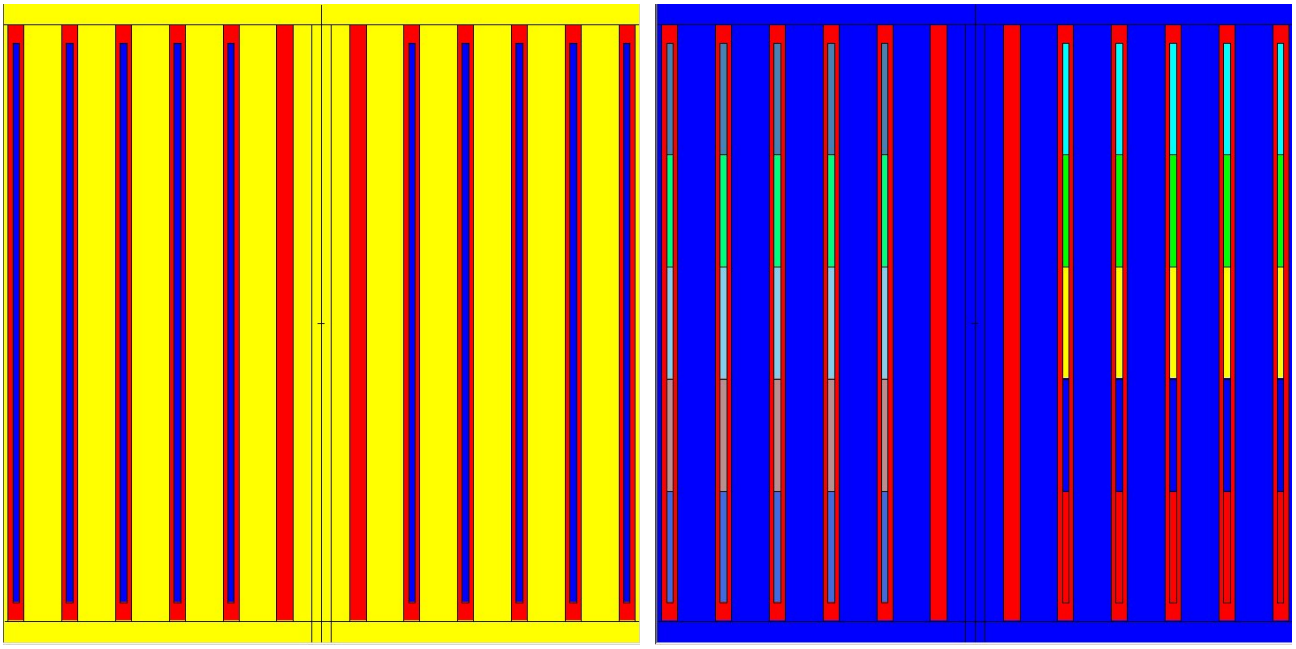

Fig. 10 Expanded XZ view of a portion of the fuel assemblies in locations D3 and D4.

Figure Notes: These two sketches (which are not to scale) show the reference (left side) versus depletion-ready (right side) zone layouts for the fuel meat regions. The material order is different so the base colors have changed, but the specifications for a 1-material/region vs. multiple-material/region layout is clearly visible in these localized snapshots.

that builds up during the actual run. Detailed analysis of the 50 MWD core configuration is currently a "work-in-progress", so no formal results/conclusions are available as yet. However, the current (July 2011) critical blade heights in the model match those of the real reactor quite accurately, with a "critical" k-value of about 0.996 -- and this gives us some confidence that the fuel depletion effects over 50 MWD of operation have been treated reasonably well.

Summary Status of the MCNP UMLRR Models

To briefly summarize the current status of the UMLRR MCNP modeling effort, we feel that the actual MCNP model is essentially complete. The critical configurations for the M-1-3 startup core, a BOL representation of the M-2-5 core, and a reasonable approximation to the July 2011 M-2-5 core with nearly 50 MWD of burnup, all give good results for the "critical" reactivity level of the system, as summarized in Table 1. Note also that both the reference and depletion-ready BOL M-2-5 models give essentially the same result -- as they should. Furthermore, we have done a number of preliminary evaluations to compare experimental and computational results for all the control and regulating blade worths in all three cores, for some axial thermal flux profiles in the M-1-3 core, and for some reactivity tests in the M-1-3 and July 2011 M-2-5 configurations -- and all these results were quite reasonable. At present, we are currently performing all these calculations one last time with the "final" versions of each of the core models, and will hopefully have a complete set of "final" results compiled within a few weeks (these calculations are extremely computer intensive, especially when considering the many MCNP cases that are needed to develop the blade worth curves -- 12-13 runs for each blade for five blades and three configurations leads to nearly 200 separate MCNP runs). In addition, a detailed analysis of the depleted core relative to a similar core configuration that uses fresh fuel compositions is underway -- and this study will tell

us whether or not the more complex depletion-capable models are really needed. Thus, with a concentrated computational effort over the next several weeks, we should have all the results needed to formally validate the final MCNP models and to bring this modeling project to closure.

Table 1 Summary results for several critical configurations within the UMLRR.

Model Description	Blades 1-4 Location (inches out)	Regulating Blade Location (inches out)	Computed "Critical" K_{eff}	Standard Deviation (20M histories)
BOL M-1-3	15.3	8.0	0.99498	0.00017
BOL M-2-5	14.9	10.0	0.99869	0.00018
BOL M-2-5 (depletion ready)	14.9	10.0	0.99838	0.00017
M-2-5 at 50 MWD	16.3	7.7	0.99563	0.00017

The Co-60 Irradiation Facilities

In addition to the MCNP modeling of the UMLRR, another subtask associated with this overall project involves modeling of some of the Co-60 irradiation facilities within the UMass-Lowell Radiation Laboratory. Specifically, we were tasked with the generation of two MCNP models -- one containing a standard Co-60 rack within a large water volume, and another which contains the same rack integrated with the UMLRR gamma cave geometry. The rack + water model is essentially complete and this is described briefly below, but we are only in the initial stages of setting up the rack + gamma cave model. Thus, the second model will have to be described and interpreted in later documentation.

Concerning the rack + water model, this is simply a standard Co-60 rack, sitting on a 1″ thick aluminum plate, in a large pool of water. The origin of the system is in the center of the rack geometry and the overall rack dimensions are approximately 9.75″ × 0.625″ × 19.1″ in the x, y, and z directions, respectively. Thus, since the thin dimension is placed along the y-axis, the relatively thin rack represents a gamma source with dimensions of about 9.75″ × 19.1″ in the xz plane. The surrounding water region extends 3 ft on both sides of the origin in the x and z directions and, in the y direction, it extends 2 ft behind the rack and 6 ft in front of the rack. Of interest here is the total gamma flux as a function of position from the rack center, with primary focus on its attenuation versus distance in the +y direction.

The rack itself, as shown in Figs. 11 and 12, contains 18 possible pencil locations, but typically only 16 locations have active Co-60 pencils inserted, with the two center locations left empty to help flatten the resultant gamma flux profile in the vicinity of the rack. The outer SS316 structure secures the individual pencils in the desired locations and creates a rigid rack geometry that allows easy handling and placement of the rack in various irradiation facilities (i.e. this same rack was used for the gamma cave irradiations as well as for the rack-in-pool tests).

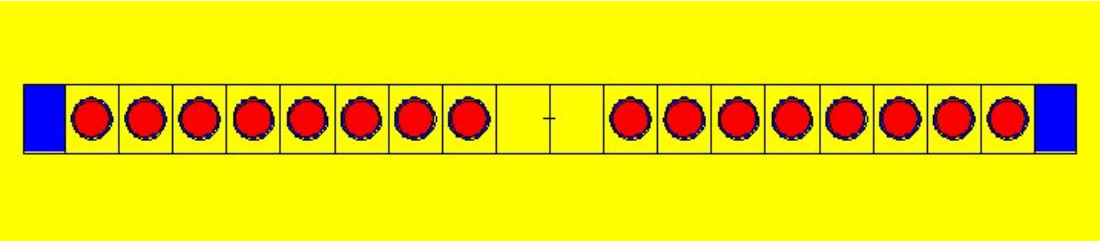

Fig. 11 Top view (xy plane) of MCNP model for the Co-60 rack (z = 0).

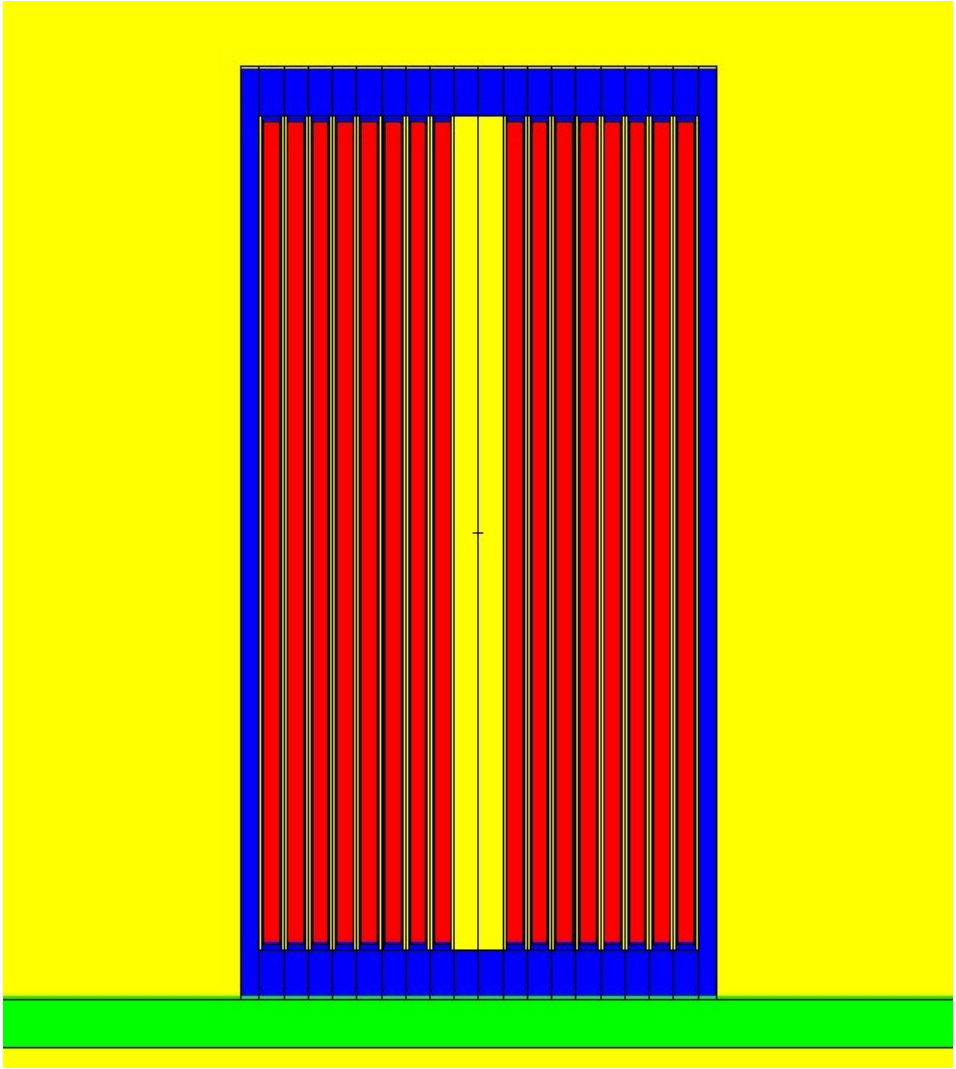

Fig. 12 Side view (xz plane) of MCNP model for the Co-60 rack (y = 0).

The active pencils are C-188 Co-60 sealed sources obtained from MDS Nordion and, unfortunately, some of the details of the pencil design are considered proprietary -- thus, some assumptions about the internal dimensions and physical layout were required. The external pencil dimensions were specified and the relative placement of the internal 14 cobalt slugs were given, with six active Co-60 slugs (red) and 8 inactive slugs (yellow) placed as shown in the rough sketch to the right (sketch is not to scale). However, information about the exact dimensions of the slugs, how they were encased, etc. was not available. Thus, we assumed that everything interior to the SS316 capsule is pure cobalt with a slug height of 1.2″ and an outer diameter of 0.33″. Note that, with this assumption, the axial layers indicated in the sketch that separate the individual slugs are not really needed since the material composition is assumed to be the same for each slug. In contrast, however, the discrete axial placement of the gamma sources in only the active slug locations is indeed important, but this is more easily handled with the source description input to MCNP rather than with the geometry specifications. Thus, the explicit axial layering implied in the sketch is not included in the MCNP geometry model (as apparent in Fig. 12).

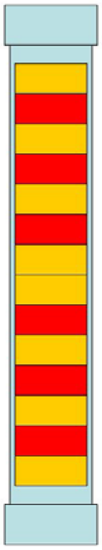

The total Co-60 activity of each pencil is specified when purchased from the supplier and each pencil is tagged so that its activity versus time can be tracked. The rack used in the experimental testing done in late October 2010 was Co-60 Rack C-2 and the activity level by pencil for that particular rack on that specific test date has been incorporated directly into the MCNP source specifications. The total source activity for Rack C-2 at the end of Oct. 2010 was about 19.9 kCi and this translates to a total gamma source strength of about 1.472e15 gammas/sec. This value was used to normalize the resultant gamma fluxes per source particle that is output from MCNP to give an absolute flux level in particles/cm^2-sec.

Although only limited testing of the model has been completed to date, an MCNP fmesh tally over a 3-D grid surrounding the rack gives results that seem quite reasonable for the current relatively simple source-in-water layout. In particular, the fmesh tally results over a 5 cm grid are displayed in Figs. 13 – 15 in a variety of formats (note that Δy was increased to 10 cm beyond y = 80 cm).

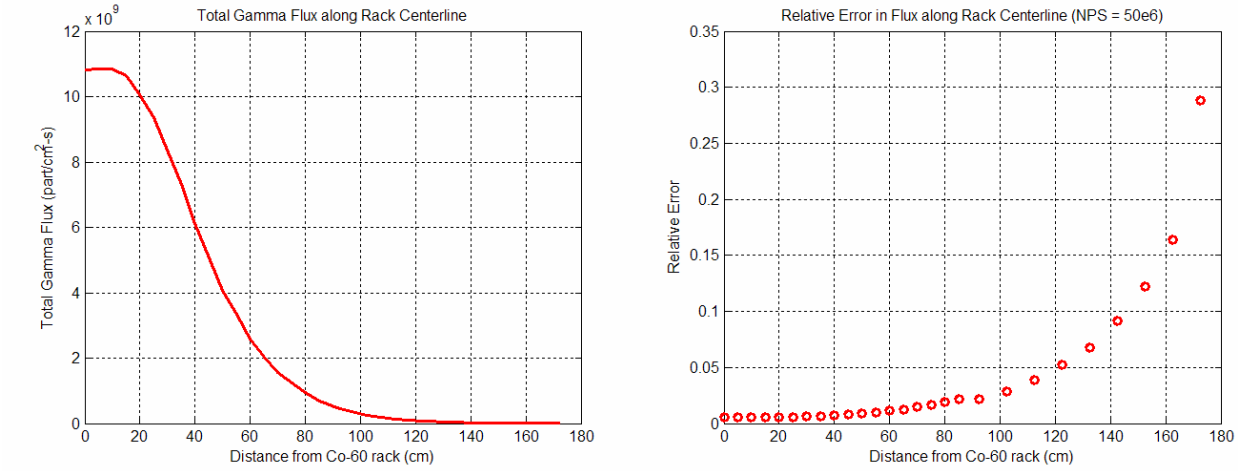

Fig. 13 Gamma flux and fractional error vs. y along the rack centerline.

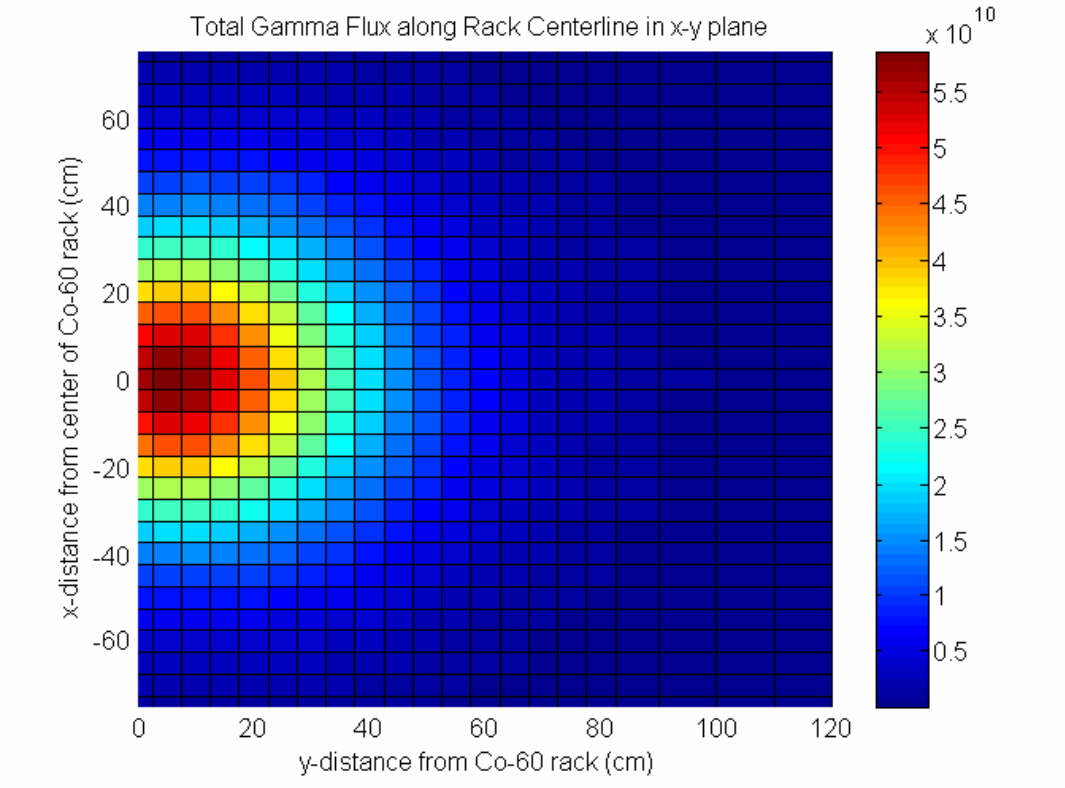

Fig. 14 Gamma flux distribution in the xy plane at z = 0.

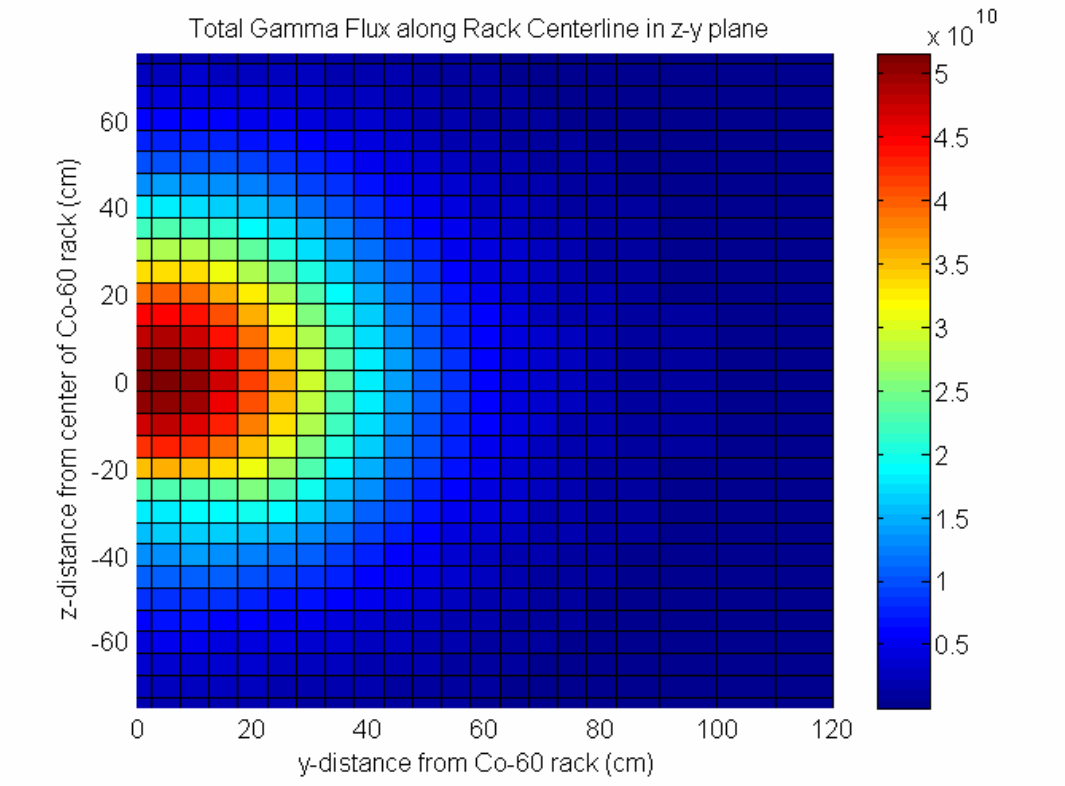

Fig. 15 Gamma flux distribution in the zy plane at x = 0.

Specifically, Fig. 13 shows that, after about 30-40 cm from the rack face, the flux attenuates as expected in a nearly pure exponential fashion and, as the tally volumes become further removed from the source, the fractional error begins to grow exponentially (again as expected). Close to the source, that spatial dependence is flatter and it depends more on the multidimensional nature of the source-detector orientation. Basically, however, there are no surprises here.

Figures 14 and 15 show the same basic trends, but this time, 2-D surface plots in the xy and zy planes are shown at the centerline of the rack in the transverse direction. These profiles again show the expected attenuation with distance from the source. Figure 14 shows near perfect symmetry in the positive and negative x directions, since the model is indeed symmetric about the zy plane at x = 0. However, in Fig. 15, there is some noticeable asymmetry due to the aluminum plate that support the rack on the -z side of the origin. Thus, the qualitative behavior observed here is easily explained, giving some measure of credibility to the base models. However, since no measured data are available for this geometry, no further benchmarking can be done at this time -- this will have to wait until the rack + gamma cave model is complete, since measured data are indeed available for this configuration.

Future Work

Well, we are getting close to the formal end of this project -- officially ends on Aug. 31, 2011. There is still a lot of work left to be completed, but it appears that most of the needed calculations can indeed be completed by this end date. We are currently in production mode in terms of completing final calculations for the MCNP reactor models and these computations and analyses should be complete in 2-3 weeks. The MCNP gamma cave model with the same rack and source specifications as described above has only been recently started, but it should not take too long to complete the geometry modeling for this system. Validating the model, on the other hand, can potentially be a time-consuming effort, since interpreting the experimental results within the computational framework is often problematic -- and we have not previously attempted to model the gamma cave and interpret the available measured data. Hopefully this will go smoothly so that there are no significant delays in completing this portion of the work.

Concerning final documentation, it will indeed take some time beyond the official end date to complete a formal final report for this project. However, informal results can be transmitted soon after generation, so a delay in the formal final documentation should not hold up application of the models, results, and conclusions of this work. The final project report will be completed as soon as possible within the time constraints associated with completing the model validation efforts and within the time constraints associated with the start of a new academic in about three weeks.

References

1. J. R. White, “Progress Report on MCNP Modeling for the UMLRR,” informal in-house project documentation (Nov. 2010).
2. “J. R. White and R. Gocht, “Progress Report on MCNP Modeling for the UMLRR,” informal in-house project documentation (Jan. 2011).
3. J. R. White, “Project Summary on MCNP Modeling for the UMLRR and Selected Gamma Irradiation Facilities,” informal presentation given at the Naval Undersea Warfare Center, Newport , RI (March 2011).

4. J. R. White, A. Jirapongmed, L. Bobek, and T. M. Regan, “Design and Initial Testing of an Ex-Core Fast Neutron Irradiator for the UMass-Lowell Research Reactor,” 2002 ANS Radiation Protection and Shielding Topical Conference, Santa Fe, NM (April 2002)
5. J. R. White, L. Bobek, and T. M. Regan, “Initial Testing of the New Ex-Core Fast Neutron Irradiator at the UMass-Lowell Research Reactor,” informal in-house project documentation (June 2002).
6. Z. Xu and P. Hejzlar, “MCODE, Version 2.2: An MCNP-ORIGEN Depletion Program,” MIT-NFC-TR-104, MIT Center for Advanced Nuclear Energy Systems (December 2008).